Redox Properties of the Iron Complexes of Orally Active Iron Chelators *CP20*, *CP502*, *CP509*, and *ICL670*

by **Martin Merkofer**[a]), **Reinhard Kissner**[a]), **Robert C. Hider**[b]), and **Willem H. Koppenol***[a])

[a]) Laboratorium für Anorganische Chemie, Departement Chemie und Angewandte Biowissenschaften, ETH-Hönggerberg, CH-8093 Zürich (e-mail: koppenol@inorg.chem.ethz.ch)

[b]) Department of Pharmacy, King's College London, Franklin-Wilkins Building, 150 Stamford Street, London SE1 9NN, UK

Redox cycling of iron is a critical aspect of iron toxicity. Reduction of a low-molecular-weight iron(III)-complex followed by oxidation of the iron(II)-complex by hydrogen peroxide may yield the reactive hydroxyl radical ($OH^{\bullet}$) or an oxoiron(IV) species (the *Fenton* reaction). Complexation of iron by a ligand that shifts the electrode potential of the complex to either to far below -350 mV (dioxygen/superoxide, pH = 7) or to far above $+320$ mV ($H_2O_2/HO^{\bullet}$, H_2O pH = 7) is essential for limitting *Fenton* reactivity. The oral chelating agents *CP20*, *CP502*, *CP509*, and *ICL670* effectively remove iron from patients suffering from iron overload. We measured the electrode potentials of the iron(III) complexes of these drugs by cyclic voltammetry with a mercury electrode and determined the dependence on concentration, pH, and stoichiometry. The standard electrode potentials measured are -620 mV, -600 mV, -535 mV, and -535 mV with iron bound to *CP20*, *ICL670*, *CP502*, and *CP509*, respectively, but, at lower chelator concentrations, electrode potentials are significantly higher.

Introduction. – Excessive amounts of iron in the body are toxic, probably through the catalytic generation of oxy radicals [1]. Chronic iron overload arises in several clinical conditions, *e.g.*, after blood transfusions for the treatment of certain anemias, and is presently managed by chelation with the bacterial siderophore desferrioxamine. However, desferrioxamine cannot be taken orally and must be injected. The successful design of a non-toxic selective iron chelator that can be administered orally has become a primary goal of research in the field of iron-overload diseases. The ideal iron chelator is one that is specific for iron with high affinity, forms an inert complex, is bioavailable, and has low toxicity [2].

Redox cycling of iron is considered essential for its toxicity. Reduction of a low-molecular-weight Fe^{III}-complex followed by oxidation of the Fe^{II}-complex by H_2O_2 yields the reactive hydroxyl radical ($OH^{\bullet}$) or an oxoiron(IV) species (the *Fenton* reaction). These species may initiate radical chain reactions that cause far more damage than the initiating event [3][4]. The Fe^{III}-complex of desferrioxamine exhibits no *Fenton* activity, and, therefore, may suppress iron toxicity in addition to its ability to remove iron from the body.

Complexation of iron with chelators that stabilize both Fe^{II} and Fe^{III} are capable of redox cycling, a property essential to a wide range of enzymes and industrial catalysts [5]. In contrast, the high selectivity of siderophores (catechols and hydroxamates) for Fe^{III} over Fe^{II} renders redox cycling under biological conditions unlikely. This selectivity is very large and leads to extremely low electrode potentials; *e.g.*, with

enterobactin and desferrioxamine, the values are −750 mV and −468 mV, respectively [6]. Iron complexes with N-atom donors tend to have higher electrode potentials, which may lead to redox cycling under aerobic conditions [2].

The bidentate chelating agents *CP20* (=1,2-dimethyl-3-hydroxypyrid-4(1*H*)-one; deferiprone; *L1*; **1**), *CP502* (=1,4-dihydro-3-hydroxy-*N*,1,6-trimethyl-4-oxobenzoic acid; **2**), and *CP509* (=1,4-dihydro-3-hydroxy-*N*,*N*,1,6-tetramethyl-4-oxobenzoic acid; **3**) are hydroxypyridones. They combine the characteristics of both hydroxamate and catechol groups (see **1B** and **1D** in *Scheme 1*) and form five-membered chelate rings in which the metal is coordinated by two vicinal O-atoms. The introduction of the amido function at C(2) of the 3-hydroxypyridin-4-one moiety in *CP502* enhances, compared to *CP20*, the affinity for Fe^{III} in the pH range 5–8. This enhancement is due to intramolecular stabilization of the ionized ligand species resulting from the combined effect of intramolecular H-bonding between the substituent at C(2) and the adjacent 3-OH function and the electron withdrawing effect of the pyridinone ring [7].

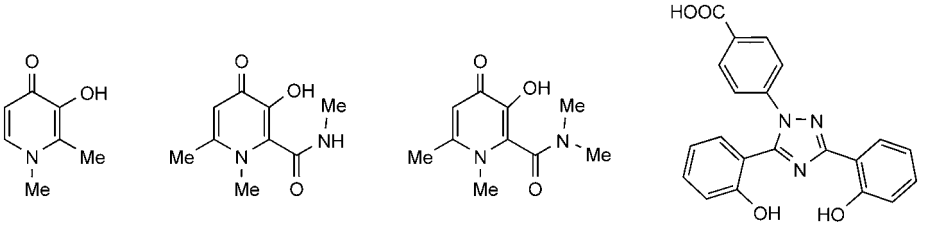

Scheme 1. *Resonance Forms of* CP20 (**1A**) *and Protonated* CP20 (**1C**) *Showing Hydroxamate-Like* (**1B**) *and Cathechol-Like* (**1D**) *Structures*

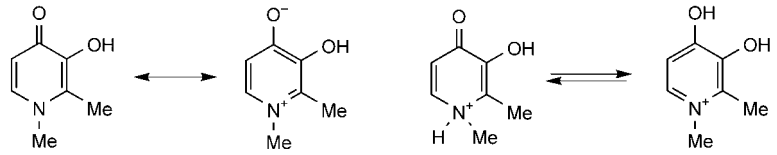

The present study was carried out to determine the electrode potentials as a function of concentration, Fe/ligand ratio, and pH of the Fe^{III}- and Fe^{II}-complexes of **1**, **2**, **3**, and *ICL670* (= 4-[3,5-bis(2-hydroxyphenyl)-1*H*-1,2,4-triazol-1-yl]benzoic acid; **4**), which are in clinical use or are intended for clinical use against iron overload diseases. The iron chelating agent *CP20* is presently already in use for the treatment of iron overload in thalassemia [8]. The chelator *ICL670* is a tridentate substituted 3,5-bis(*ortho*-hydroxyphenyl)-1,2,4-triazole. *Ryabukhin et al.* reported that compounds of this class form polymeric complexes with doubly charged transition metal ions [9].

Experimental. – *Materials.* Analytical grade *CP20* (**1**) was purchased from *Aldrich*. Chelators *CP502* (**2**) and *CP509* (**3**) were prepared by one of us (*R. C. H.*). A sample of purified *ICL670* (**4**) was kindly provided by

Prof. *K. Hegetschweiler* (University of Saarbrücken). Water was purified with a *Millipore Milli-Q* unit fed with deionized water. Analytical reagent grade $Fe(NO_3)_3 \cdot 9\,H_2O$ was used to provide Fe^{III}; the *Tris* buffer (*Sigma*), HCl, and HNO_3 (*Merck*) were also analytical grade.

Spectrophotometric Measurements. The optical absorbance spectra of the metal complex species were measured with a *Specord 200* (*Analytik*, Jena) spectrophotometer and quartz cells with an optical path length of 1.000 ± 0.001 cm. Solns. of **1** and **2** were prepared in 0.1M *Tris* buffer. Because **4** is not water soluble at neutral and acid pH, a soln. in MeOH/H_2O 1:1 was prepared. HCl was used to adjust the pH of the solns.

Cyclic Voltammetry. Electrochemical measurements were performed with an *AMEL 2049 Potentiostat* and an *AMEL 568* function generator. A glassy carbon electrode (GCE) was used as auxiliary electrode an Ag/AgCl/KCl(s) electrode as reference electrode (*Metrohm*) and a mercury electrode as working electrode (*Metrohm*). The reference electrode was connected through a ceramic frit to the cell soln. by a bridge filled with 1.5M $(NH_4)_2SO_4$. All electrochemical experiments were carried out at r.t. under an atmosphere of purified N_2. HNO_3 was used to adjust the pH of solns. All potentials in the text are *vs.* the normal hydrogen electrode (NHE).

Results. – *UV/VIS Absorbance Spectra*. We measured the pH-dependent UV/VIS absorbance spectra of the complexes to determine the species distribution, prior to cyclic voltammetry. Although we used HNO_3 to adjust the pH in the cyclic voltammetry experiments, because NO_3^- has an absorbance at 302 nm ($\varepsilon = 6\,M^{-1}\,cm^{-1}$), we used HCl instead for the UV/VIS spectra. The pK_a values of the ligands and the stability constants of Fe^{III} with these ligands are presented in *Table 1* along with the stability constants of other iron chelators.

Table 1. *pK_a Values and Stability Constants of Fe^{III} Complexes of Iron Chelators*

Ligand	pK_{a1}	pK_{a2}	pK_{a3}	log K_1	log β_2	log β_3	Ref.
CP20 (**1**)	3.62	9.76		15.14	26.68	35.92	[10]
CP502 (**2**)	2.77	8.44				34.3	[7]
ICL670 (**4**)	4.62	10.13	12.09		36.9		[11]
Catechol	9.3	~13.3		20.4	35.5	44.9	[10]
Enterobactin	9.2	12.1	12.1	~52			[10]
Transferrin				20.2	33.9		[10]
Desferrioxamine	8.32	8.96	9.55	30.99			[10]

*Iron/*CP20. Iron is coordinated by *CP20* (**1**) *via* the phenol and keto groups. It has two protonation constants (see *Table 1*) corresponding to the formation of HL and H_2L^+ (formulas **1A** and **1C**, respectively, in *Scheme 1*). *Fig. 1* shows the UV/VIS absorbance spectra obtained at the pH values indicated. The absorbance at 440 nm corresponds to the formation of the Fe^{III}/**1** 1:3 complex (FeL_3). The isosbestic point at 500 nm corresponds to the equilibrium between the Fe^{III}/**1** 1:3 and Fe^{III}/**1** 1:2 complexes. The other isosbestic point above 600 nm is ill-defined because more than two species are in equilibrium (the Fe^{III}/**1** 1:1, 1:2, and some 1:3 complexes). The lowest curves at pH 1.4 correspond almost entirely to the 1:1 complex. These results are in agreement with the cyclic voltammetry measurements presented below.

*Iron/*CP502. *CP502* (**2**) is also a bidentate ligand. The pH-dependent UV/VIS absorbance spectra of Fe^{III}/**2** complexes are shown in *Fig. 2*. The similarity in pK_a values and stability constants with Fe^{III} suggests speciation similar to that of the Fe^{III}/**1** complexes. We found again two isosbestic points: the one at 500 nm corresponds to the equilibrium between the Fe^{III}/**2** 1:3 and Fe^{III}/**2** 1:2 complexes, and the second

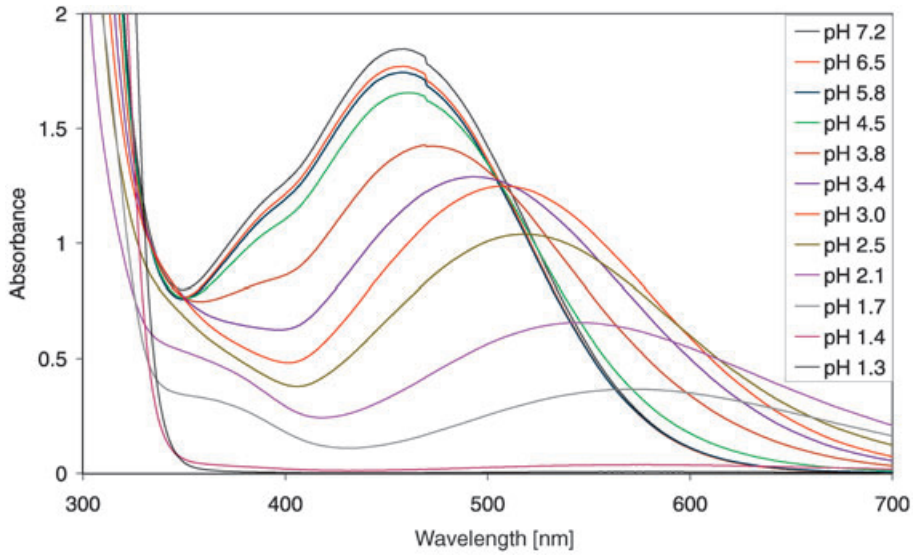

Fig. 1. *UV/VIS Spectrum of the* Fe^{III}/CP20 (**1**) *1:3 complex in 0.1*M Tris *buffer as a function of pH, as indicated.* The pH was changed by additions of HCl. Conditions: $[Fe^{III}]_0 = 0.4$ mM; $[CP20]_0 = 1.2$ mM.

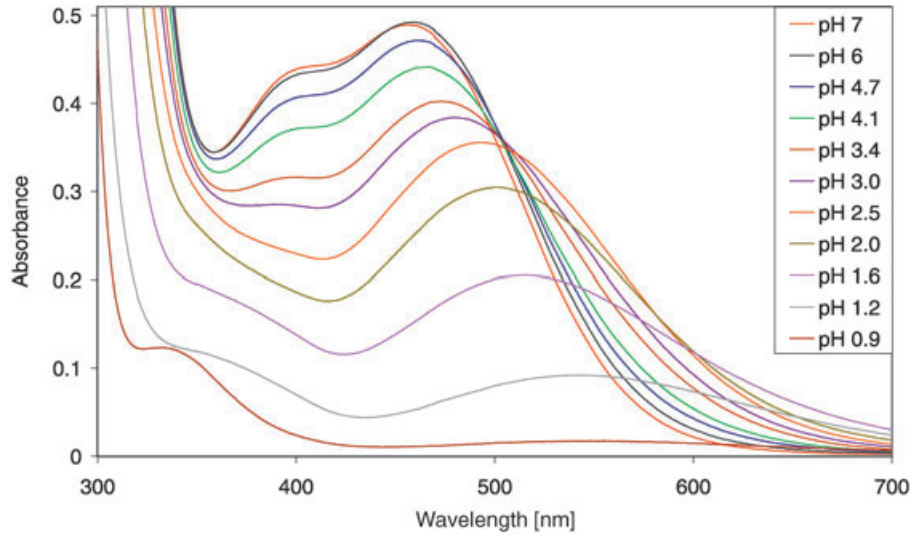

Fig. 2. *UV/VIS Spectrum of the* Fe^{III}/CP502 (**2**) *1:3 complex in 0.1*M Tris *buffer as a function of pH, as indicated.* The pH was changed by additions of HCl. Conditions: $[Fe^{III}]_0 = 0.1$ mM; $[CP502]_0 = 0.3$ mM.

diffuse isosbestic point near 600 nm indicates that more than two species are in equilibrium.

*Iron/*ICL670. *ICL670* (**4**), a tridentate ligand, is insoluble under neutral and acidic conditions; it is also insoluble in MeCN. The ligand is soluble in DMSO, but this is not a

good solvent for cyclic voltammetry. The Fe^{III}/**4** complex was, therefore, prepared in a *Tris*-buffered solution of MeOH/H_2O 1:1: the ligand and the Fe^{III} salt were dissolved in MeOH before addition of *Tris* buffer. The viscosity behavior of this mixture is similar to that of water. *Fig. 3* shows the UV/VIS absorbance spectra obtained at various pH values. The two maxima at 403 nm and 467 nm correspond to the Fe^{III}/**4** 1:2 complex ($[FeL_2]^{3-}$). The absorbance maximum at 512 nm is due to the protonated 1:1 $[FeHL]^+$-complex [11].

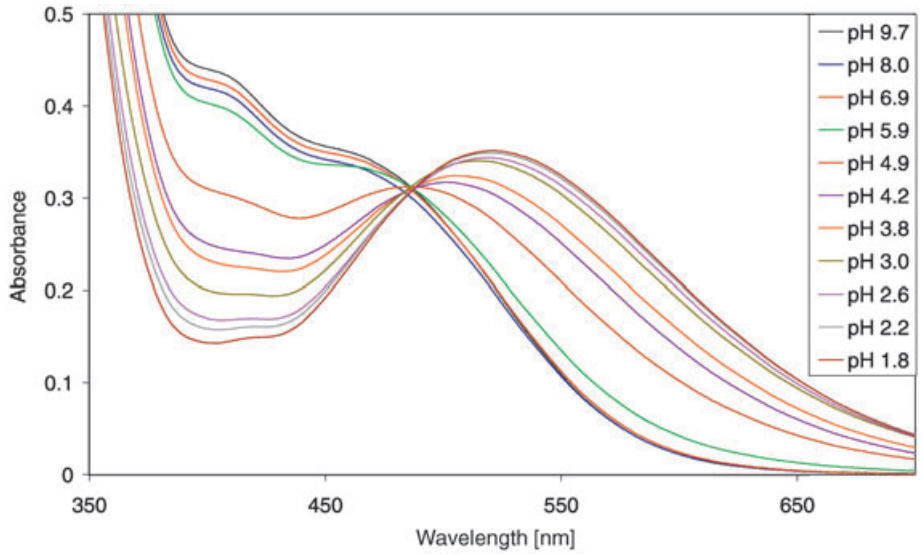

Fig. 3. *UV/VIS Spectrum of the Fe^{III}/*ICL670 (**4**) *1:2 complex in buffer as a function of pH, as indicated.* The spectrum was recorded in 0.1M *Tris* buffer in MeOH/H_2O 1:1. The pH was changed by addition of HCl. Conditions: $[Fe^{III}]_0 = 0.1$ mM; $[ICL670]_0 = 0.2$ mM.

The UV/VIS absorbance spectra for Fe^{III}/**4** show that there is, unlike with Fe^{III}/**1** and Fe^{III}/**2**, only one isosbestic point at 488 nm, which indicates a single equilibrium between two species over the pH range 1.8 to 9.7. Because the absorbance at 403 nm is constant at pH 6 and higher, we conclude that, under these conditions, only the Fe^{III}/**4** 1:2 complex is present.

*Cyclic Voltammetry. Iron/*CP20. Cyclic voltammetry was performed at different pH values as well as at different ratios of ligand to metal and at different concentrations. We also examined whether the pH at which the complexes were synthesized has an influence on the ultimate species distribution. In *Fig. 4,* voltammograms are shown as a function of the Fe^{III}/**1** ratio. For the 1:1-complex, the equilibrium potential cannot be determined because the reverse reaction is not detectable. The Fe^{III}/**1** 1:2 complex produces two peaks during the reduction and one broad one during the oxidation. We conclude that there are two species in solution, namely the 1:1 and the 1:2 complexes. With higher ligand to iron ratios, up to and above 3 equivs. of ligand, the cyclic voltammograms are reversible, and there is only a single species in solution. At higher ligand concentrations, the electrode potential becomes more negative.

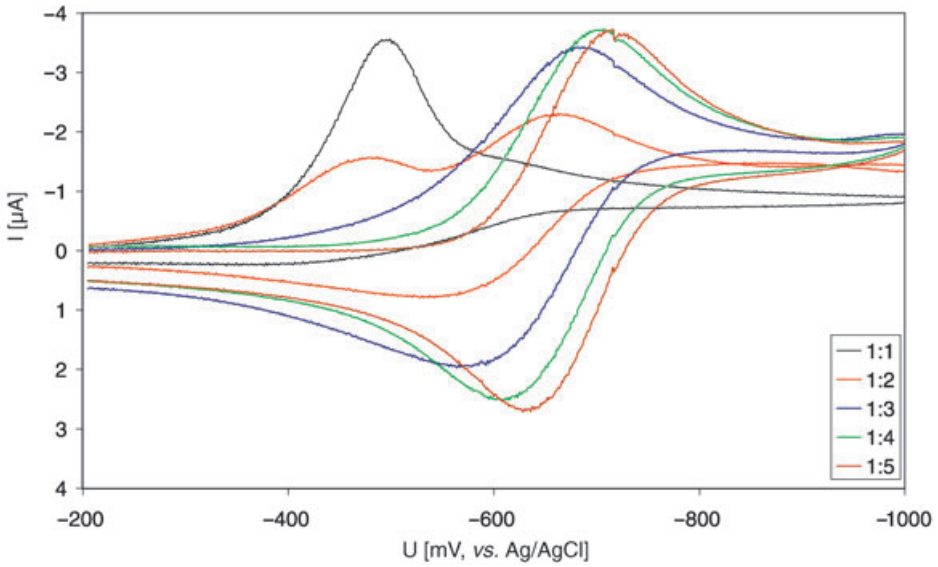

Fig. 4. *Dependence of cyclic voltammograms on the Fe/*CP20 (**1**) *ratio.* Voltammograms were recorded with a Hg electrode in 0.1M *Tris* buffer. Conditions: scan rate = 100 mV s^{-1}, $[Fe]_{total}$ = 1 mM, pH = 7.2.

Fig. 5 shows the pH dependence of the cyclic voltammetry. It is obvious that, at higher pH, the electrode potential shifts to lower values. The complexes for these measurements were formed at pH 7.2 and then brought to the desired pH by addition of HNO_3. The advantage of HNO_3 over HCl in the electrochemistry experiments is that nitrate is a weaker ligand for Fe^{III} (log $K_1 = -0.23$) than chloride (log $K_1 = 0.63$), and there is less danger that a ligand in the coordination sphere will be substituted. To find out whether these conditions have an influence on the electrode potential or on the species distribution, the complexes were synthesized at acidic pH and then brought to the desired pH with buffer. The cyclic voltammograms of both preparations are identical.

In *Fig. 6*, voltammetry as a function of Fe^{III} concentration is shown. With higher iron concentrations at the same ratio of metal to ligand, the electrode potential shifts to lower values. In *Fig. 7,* the experimental values of the electrode potentials are compared to those calculated from theory [12].

*Iron/*CP502. *Fig. 8* shows the reduction of solutions containing 0.1 mM iron and 0.6 mM *CP502*. The presence of a pre-peak indicates that this complex adsorbs to the electrode; a possible explanation for the observed electrochemical adsorption is that *CP502* is more hydrophilic than *CP20*. Furthermore, under these conditions, several species appear to be present in solution. When this solution was diluted with 0.1M *Tris* buffer to a concentration of 0.02 mM iron (0.12 mM *CP502*) and measured again, a single peak was observed upon oxidation and reduction. This experiment shows that concentration, as expected, influences adsorption of the ligand to the electrode.

The pH dependence of Fe^{III}/**2** voltammograms is shown in *Fig. 9*. Above pH 6, the peaks are symmetric, and the leading and trailing slopes both have similar inclines,

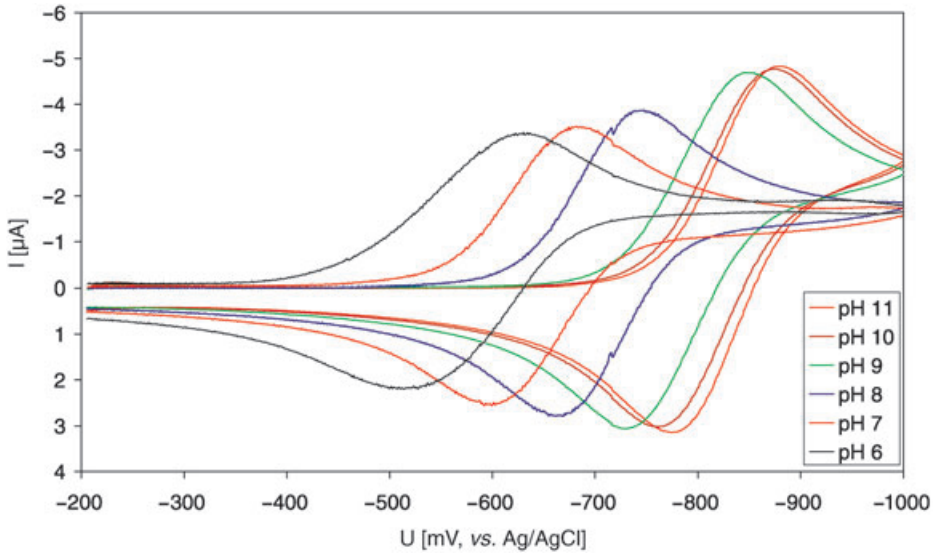

Fig. 5. *Dependence of cyclic voltammograms of Fe/*CP20 (**1**) *on pH, as indicated.* Voltammograms were recorded with a Hg electrode in 0.1M *Tris* buffer. Conditions: scan rate = 100 mV s^{-1}, $[Fe]_{total}$ = 1 mM; $[CP20]_{total}$ = 5 mM.

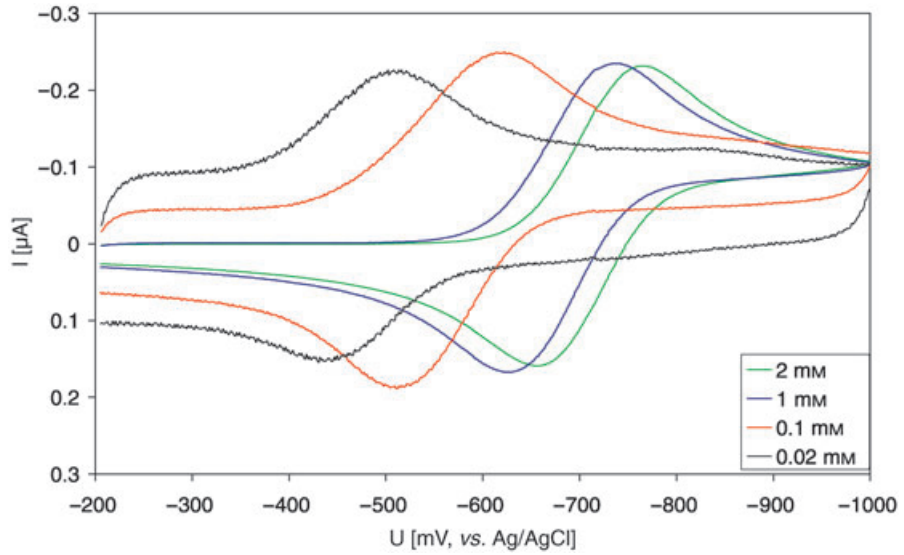

Fig. 6. *Dependence of cyclic voltammograms of Fe/*CP20 (**1**) *on Fe concentration.* Voltammograms were recorded with a Hg electrode in 0.1M *Tris* buffer. The current for each [Fe] was normalized to that of 0.02 mM Fe. Conditions: scan rate = 100 mV s^{-1}, Fe/*CP20* 1:5, pH 7.2.

which indicates adsorption [13]. However, the shape of the peak at pH 6 shows that there is no adsorption.

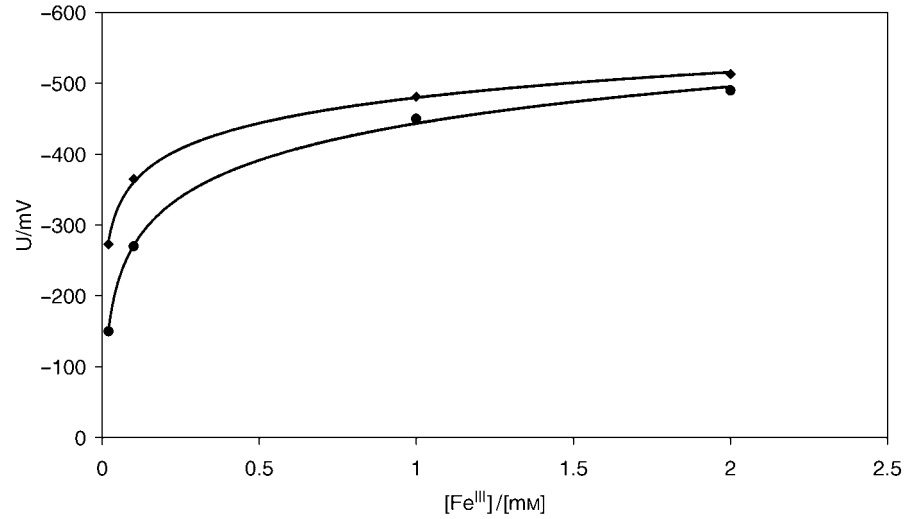

Fig. 7. *Electrode potentials as a function of [Fe^{III}]*. Conditions: Fe/*CP20* (**1**) 1:5, pH 7.2. Experimental values (◆); values calculated by means of the formula derived from *Templeton* [12] (●).

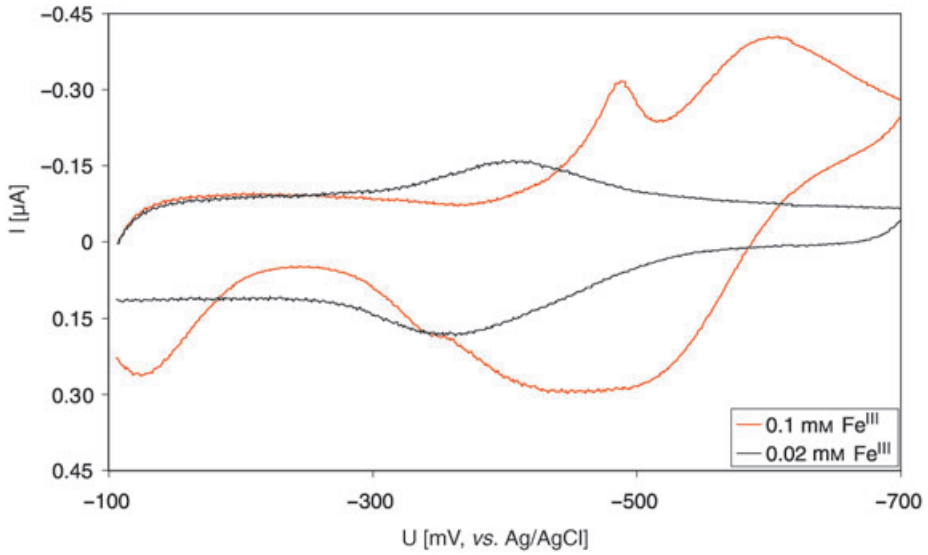

Fig. 8. *Dependence of cyclic voltammograms on the concentration of Fe/*CP502 (**2**). Voltammograms were recorded with a Hg electrode in 0.1M *Tris* buffer. Conditions: scan rate = 100 mV s^{-1}, $[Fe]_{total}$ = 0.1 mM or 0.02 mM, Fe/*CP502* 1:6, pH = 7.2.

Iron/CP509. The electrode potential of the Fe^{III}/**3** complex was measured to determine whether the presence of a second Me group at the N-atom influences electrochemical properties (*i.e.*, adsorption) compared to Fe^{III}/**2**. *Fig. 10* shows that

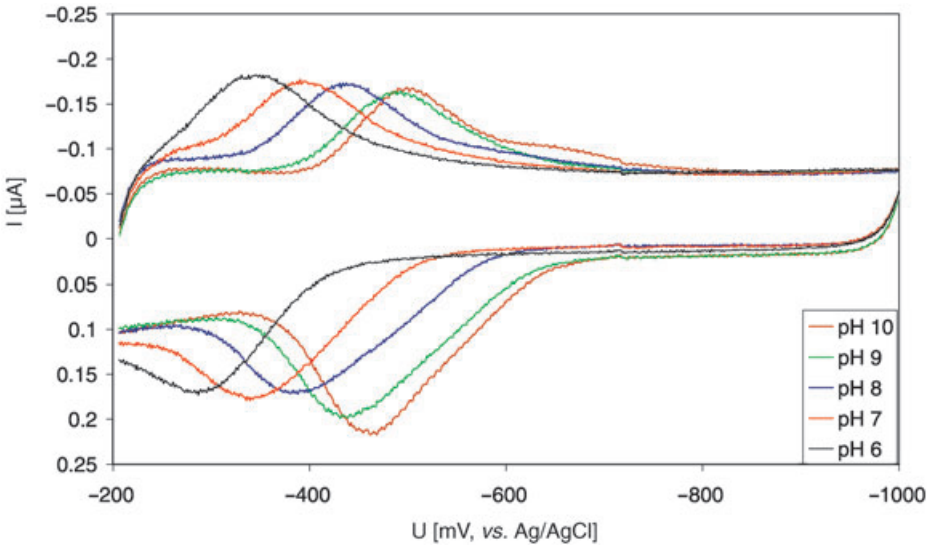

Fig. 9. *Dependence of cyclic voltammograms of Fe/*CP502 (**2**) *on pH, as indicated.* Voltammograms were recorded with a Hg electrode in 0.1M *Tris* buffer. Conditions: scan rate = 100 mV s^{-1}, $[Fe]_{total} = 0.02$ mM; $[CP502]_{total} = 0.1$ mM.

there are also adsorption phenomena above pH 6, as indicated by the symmetry of the peaks.

*Iron/*ICL670. Like in the UV/VIS experiments, the complex was prepared in MeOH, and then an equal volume of *Tris* buffer solution was added. Initial experiments with a gold electrode failed. Measurements with a mercury electrode yielded very good results, and the dependencies of the midpoint potential on pH and stoichiometry were determined.

The influence of the Fe^{III}/**4** ratio on the electrode potential is shown in *Fig. 11*. Again, the electrode potential shifts to more-negative values with excess ligand present. That there is only one species in solution at all Fe^{III}/**4** ratios is indicated by the single peak, and electron transfer is fully reversible. To obtain an extrapolated electrode potential for the Fe^{III}/**4** complex in water, the MeOH concentration was varied (*Fig. 12*), and the electrode potentials obtained were plotted as a function of MeOH (*Fig. 13*). A value of -399 mV at pH 7.2 and 25° with ligand present in excess was obtained.

Ligand **4** is soluble in water under alkaline conditions. To determine whether the electrode potential is the same as that determined by varying the MeOH concentration, the ligand was dissolved in 0.1M *Tris* buffer at pH 10, the Fe^{III} salt was added, and the solution was adjusted to the desired pH with HNO_3. The electrode potential determined at pH 7.2 and 25° with excess ligand was -392 mV. To determine whether the buffer has an influence on the electrode potential, the determinations were repeated with borate buffer; the result obtained was the same as for *Tris* buffer.

The pH dependence of Fe^{III}/**4** voltammograms shows the same trends as found for the Fe^{III}/**1** and Fe^{III}/**2** complexes (data not shown): at higher pH, the electrode potential moves to more-negative values. Comparison of the species distribution with the

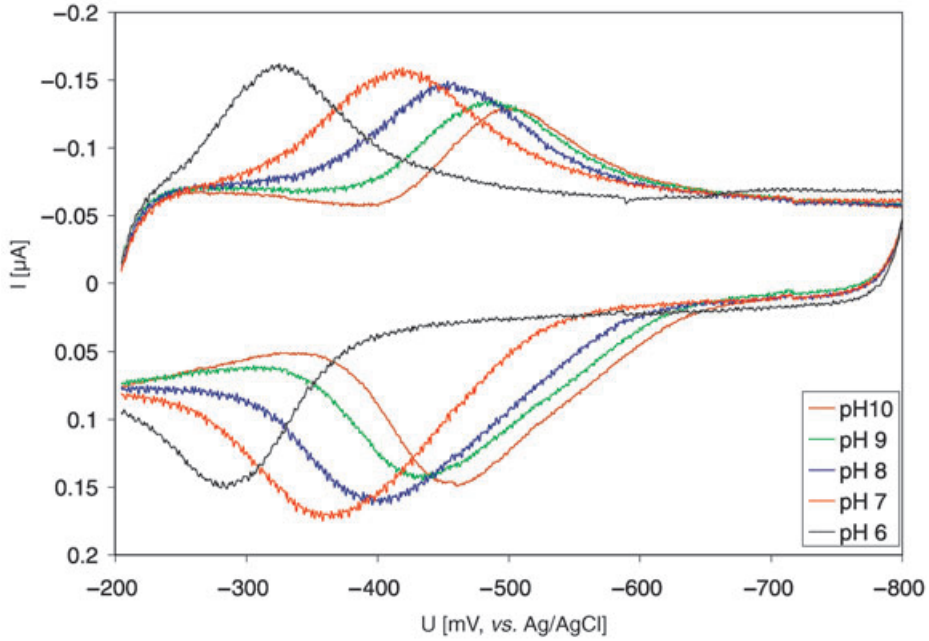

Fig. 10. *Dependence of cyclic voltammograms of Fe/*CP509 (**3**) *on pH, as indicated.* Voltammograms were recorded with a Hg electrode in 0.1M *Tris* buffer. Conditions: scan rate = 100 mV s^{-1}, $[Fe]_{total}$ = 0.02 mM; $[CP509]_{total}$ = 0.1 mM.

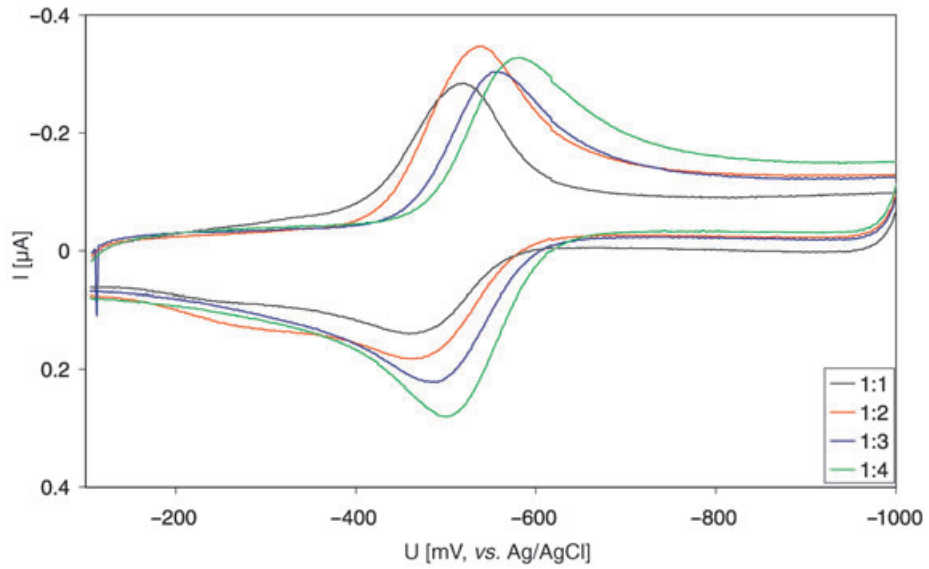

Fig. 11. *Dependence of cyclic voltammogram on the Fe/*ICL670 (**4**) *ratio.* Voltammograms were recorded with a Hg electrode in 0.1M *Tris* buffer in MeOH/H_2O 1:1. Conditions: scan rate = 100 mV s^{-1}, $[Fe]_{total}$ = 0.1 mM, pH = 7.2.

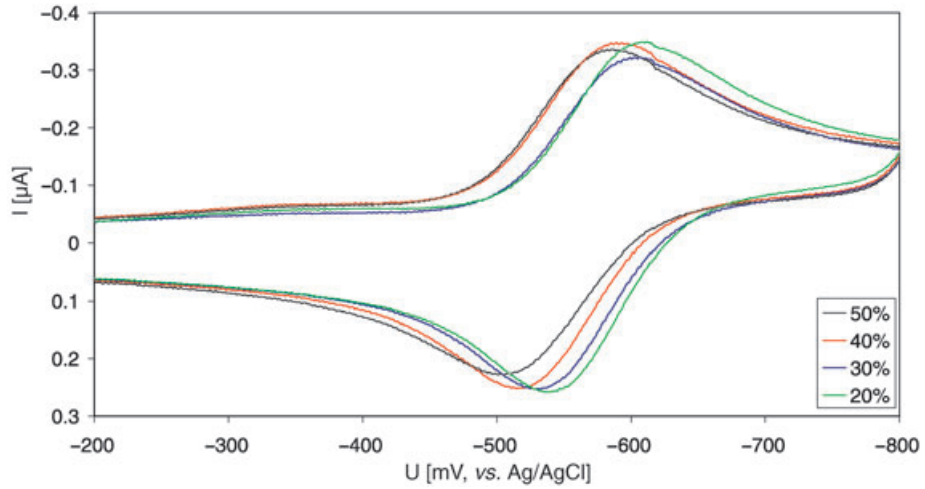

Fig. 12. *Dependence of cyclic voltammograms of Fe/*ICL670 (**4**) *on the MeOH concentration, as indicated.* Voltammograms were recorded with a Hg electrode in 0.1M *Tris* buffer in MeOH. Conditions: scan rate = 100 mV s^{-1}, $[Fe]_{total} = 0.1$ mM, $[ICL670]_{total} = 0.4$ mM, pH = 7.2.

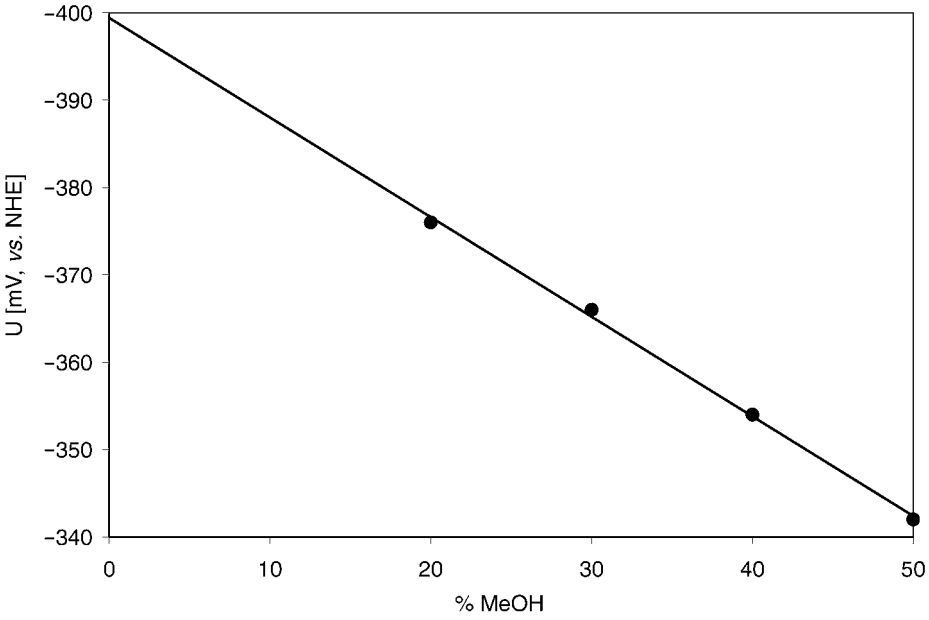

Fig. 13. *Extrapolation of the electrode potentials of Fe/*ICL670 (**4**) *as a function of [MeOH] to [MeOH] = 0*

UV/VIS spectra confirms that a single species, *i.e.*, Fe^{III}/**4** 1:2 ($[FeL_2]^{3-}$) is in solution over the pH range of 6–9.

Calculation of Stability Constants for the Fe^{II}-Complexes of **1**, **2**, *and* **4**. To calculate the stability constants of the Fe^{II}/*CP20*, Fe^{II}/*CP502*, and Fe^{II}/*ICL670* complexes, the thermodynamic cycle in *Scheme 2* was used. The stability constants of the Fe^{II}-complexes of the three ligands are known (see *Table 1*). The electrode potentials and the calculated Fe^{II} stability constants are listed in *Table 2*. The electrode potentials shown were determined at pH values where the Fe^{II} complex is completely formed. The electrode potentials of the Fe/*CP502* and Fe/*CP509* complexes are extrapolated.

Scheme 2. *Thermodynamic Cycle for the Calculation of the Fe^{II}*/CP20 (**1**) *Stability Constant*

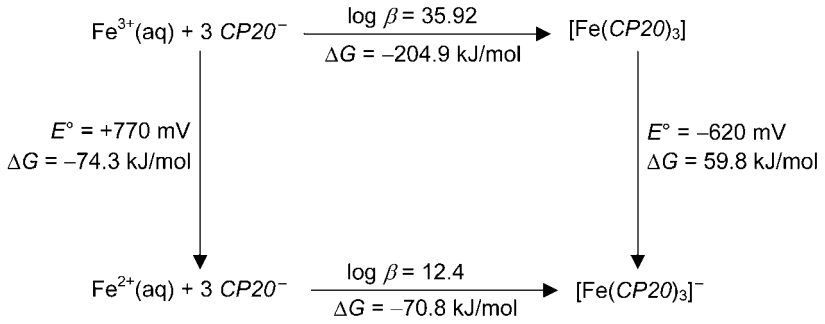

Table 2. *Electrode Potentials and Stability Constants of Fe^{II} Complexes of* **1**–**4** *at pH 11*

Ligand	Temp. [°]	E° [mV]	log β
CP20 (**1**)	25	– 620	12.4
CP502 (**2**)	25	– 535	12.2
CP509 (**3**)	25	– 535	–[a])
ICL670 (**4**)	25	– 600	13.7

[a]) Not determined.

Discussion. – To evaluate the three ligands *CP20* (**1**), *CP502* (**2**), and *ICL670* (**4**) for medicinal use, it is important to consider the oral bioavailability, the pFe^{3+} values, the toxicity, and the electrode potentials. With respect to the *Lipinski* parameters [7], which deal with oral bioavailability, all three ligands are good candidates: *i*) the molecular weights are all smaller than 500; *ii*) the log *P* (water/octanol) is < 5 in each case; and *iii*) each ligand has fewer than five H-bond donors and fewer than ten H-bond acceptors. The pFe^{3+} value at pH 7.4, calculated for total [ligand] $= 10^{-5}$ M and total [iron] $= 10^{-6}$ M was superior for *CP502* at 21.7 compared to 19.4 for *CP20* [7], even though the stability constant of the Fe^{III}/*CP20* complex is higher. The explanation is that the phenol moiety of *CP502* has a smaller pK_a value than that of *CP20*, and, therefore, more *CP502* is deprotonated at pH 7.2.

As mentioned in the *Introduction*, redox cycling is an important factor in iron toxicity. Cycling implies accessibility of a peroxide to the iron – the reaction proceeds by an innersphere mechanism – and electron transfer that is thermodynamically allowed. As shown here, the electrode potential is strongly dependent on complex concentration. The electrode potentials for the iron complexes of *CP20* and *ICL670* at

0.1 mM iron and pH 7.2 with excess ligand are -377 mV and -392 mV, respectively. At 1 mM iron and pH 11, these electrode potentials are -620 mV and -600 mV, respectively. The electrode potentials of the iron complex of *CP502* cannot be measured at 0.1 mM iron because of adsorption phenomena; for that reason, we extrapolated the value at 0.02 mM iron with the values measured for the iron complex of *CP20*. We obtain an extrapolated electrode potential for *CP502* at 0.1 mM iron and pH 7.2 with excess ligand of -292 mV. The extrapolation to 1 mM iron and pH 11 gives a electrode potential of -535 mV.

The electrode potential of the Fe^{II}/*CP20* complex is lower than that of the Fe^{II}/*CP502* complex (see *Table 2*). We assume that Fe^{II} coordinates to the phenolate and the amide groups. In the case of *CP502*, a softer donor atom is available to stabilize the Fe^{II}. This N-atom is also present in *CP509*, but the electrode potential of the Fe^{III}/Fe^{II} couple is higher than that of the *CP20* couple. Since the addition of a second Me group, as in *CP509*, does not change the electrode potential relative to that of *CP502*, it would seem likely that the second Me group does not inhibit coordination of the N-atom to Fe^{II}.

It is clear for all three ligands that the electrode potential decreases with increasing pH, probably due to involvement of the phenolate group as a donor for Fe^{III}. Calculations of the Fe^{III}/Fe^{II} couples with *CP20* and *CP502* at an iron to ligand ratio of 1:5 show that the Fe^{III} complexes are fully formed down to pH 5. In contrast, it appears that the Fe^{II} complexes are fully formed only at higher pH values (10–12) since the cyclovoltammograms show no further shifts to more-negative values above pH 10. It seems likely that, below pH 10, the reduction of the Fe^{III}-complexes is concomitant with dissociation of ligand.

At lower concentrations of ligand and iron, we found an increase in the electrode potential (see *Fig. 6*). With *CP20* ligand present in excess, *e.g.*, the potential changes from -514 mV at pH 7.2 and 2 mM Fe to -377 mV at pH 7.2 and 0.1 mM Fe. Thus, under physiological conditions, namely μM concentrations of Fe and chelator, even higher (less negative) values are expected, as implied by *Fig. 7*. However, the electrode potentials of redox couples that involve oxygen radicals increase under physiological conditions. For instance, for conditions estimated to be valid under physiological conditions, $[O_2] = 10^{-5}$ M and $[O_2^{\bullet-}] = 10^{-10}$ M, the electrode potential does not have the standard value of -350 mV, but $+136$ mV [14]. That the ligands exhibit higher electrode potentials under physiologically relevant conditions may seriously impact medicinal efficacy. The issues surrounding the electrode potentials of these ligands and their physiological relevance will be addressed in a future report.

This work was supported by the ETH Zürich, *Swiss National Science Foundation*, EU (QLK1-CT-2002-00444) and BBW (01.0397)

REFERENCES

[1] B. Halliwell, J. M. C. Gutteridge, *Methods Enzymol.* **1990**, *186*, 1.
[2] Z. D. Liu, R. C. Hider, *Coord. Chem. Res.* **2002**, *232*, 151.
[3] R. Crichton, 'Inorganic Biochemistry of Iron Metabolism', John Wiley & Sons, Ltd, Chichester, 2001, p. 235–257.
[4] W. H. Koppenol, in 'Chemical Toxicology', Ed. K. B. Wallace, Raven Press, New York, 1997, p. 3–14.
[5] G. J. P. Britovsek, V. C. Gibson, D. F. Wass, *Angew. Chem., Int. Et.* **1999**, *38*, 429.

[6] K. N. Raymond, G. Müller, B. F. Matzanke, in 'Structural Chemistry', Ed. F. L. Boschke Springer-Verlag, Berlin, **1984**, p. 49 – 97.
[7] R. C. Hider, Z. D. Liu, *Curr. Med. Chem.* **2003**, *10*, 1051.
[8] M. Y. Moridani, P. J. O'Brien, *Biochem. Pharmacol.* **2001**, *62*, 1579.
[9] Y. I. Ryabukhin, N. V. Shibaeva, A. S. Kuzharov, V. G. Korobkova, A. V. Khokhlov, A. D. Garnovskii, *Sov. J. Coord. Chem. (Engl. Transl.)* **1987**, *13*, 493.
[10] R. J. Motekaitis, A. E. Martell, *Inorg. Chim. Acta* **1991**, *183*, 71.
[11] U. Heinz, K. Hegetschweiler, P. Acklin, B. Faller, R. Lattmann, H. P. Schnebli, *Angew. Chem., Int. Ed.* **1999**, *38*, 2568.
[12] A. El-Jammal, D. M. Templeton, *Inorg. Chim. Acta* **1996**, *245*, 199.
[13] A. P. Brown, F. C. Anson, *Anal. Chem.* **1977**, *49*, 1589.
[14] W. H. Koppenol, J. Butler, *Adv. Free Radical Biol. Med.* **1985**, *1*, 91.

Received July 1, 2004